JOURNAL OF APPLIED ELECTROCHEMISTRY 19 (1989) 813–818

A.c. impedance of niobium triselenide cathode in secondary lithium cells

B. V. RATNAKUMAR, S. DI STEFANO, C. P. BANKSTON

Jet Propulsion Laboratory, California Institute of Technology, Pasadena, CA 91109, USA

Received 9 November 1988

Niobium triselenide is one of the cathode materials being evaluated at JPL for ambient temperature secondary lithium batteries for space applications. The mechanism of reduction of $NbSe_3$ involves two steps, 1 mole of Li intercalating in the first step and 2 moles of Li intercalating at lower potentials in the second step. The a.c. impedance behaviour of the $NbSe_3$ cathode under various conditions, i.e. at different reduction potentials, after discharges at various d.c. potentials and after charge/discharge cycling is discussed.

1. Introduction

Niobium triselenide has several attractive features as a cathode material in ambient temperature lithium rechargeable cells such as high gravimetric and volumetric energy densities, rugged layered structure, fibrous morphology and good electronic conductivity [1–6]. Niobium triselenide could thus be a viable cathode material in secondary lithium cells especially for space applications. In our previous communications, we reported studies on the characterization and performance of $NbSe_3$ and also the mechanism of intercalation of (three moles of) lithium with $NbSe_3$ elucidated from various electrochemical techniques [7, 8].

Niobium triselenide undergoes a topotactic reversible intercalation reaction with 3 moles of lithium. Detailed studies were made by us using various electrochemical technqiues to understand the mechanism of intercalation, i.e. whether the intercalation of 3 moles of Li occurs in a single step or in discrete steps. D.c. cyclic voltammetric curves at slow scan rates show two peaks between 2.3 and 1.2 V vs Li^+/Li. Coulometric (potentiostatic) discharges at various reduction potentials reveal two peaks in the above potential range, the first peak ranging from 2.3 to 1.7 V and the second from 1.7 to 1.55 V. The relative peak heights correspond to approximately 1 mole of Li for the first peak and 2 moles of Li for the second peak. A.c. voltammograms also exhibit two peaks at the same potentials as above suggesting two reversible steps in the reduction of $NbSe_3$. Finally, complex plane impedance plots contain two relaxation loops attributed to each of the above steps. The two-step intercalation of Li at two different sites of $NbSe_3$ is consistent with the structure of $NbSe_3$ which has two different units of chains of selenium trigonal prisms comprising two and four chains, respectively [9]. A.c. impedance measurements carried out at different states of charge [10] lend further support to the two-step intercalation in the reduction of virgin $NbSe_3$. The exchange current densities for the first and second step show peaks at different states of charge separated by more than 0.6 mole of Li.

The kinetics of reduction of $NbSe_3$ are essentially dictated by the slow mass transfer processes as evident from a current plateau in the d.c. cyclic voltammetry, limiting current and mass transfer effects in the d.c. potentiodynamic polarization and a low frequency linear regime in the Nyquist plot. The slow mass transfer process is attributed to the solid state diffusion of Li^+ ion in the $NbSe_3$ lattice.

In order to have further insight into the mechanism of intercalation, we carried out a.c. impedance studies on virgin $NbSe_3$ at different d.c. potentials and also under equilibrium conditions after coulometric (potentiostatic) discharges at various reduction potentials. Also, impedance measurements were made on laboratory prismatic test cells as a function of charge–discharge cycle to obtain a correlation with the modes of cell failure.

2. Experimental details

Niobium triselenide cathode material was synthesized as described earlier [7, 8]. Prismatic cathodes of $NbSe_3$ were made by containing (and pressing) $NbSe_3$ mat between two expanded Ni (Exmet) screens. Lithium counter and reference electrodes were made by pressing high purity Li foil (Foote Chemical Co.) onto a Ni (Exmet) screen. A prismatic three-electrode glass cell, wherein adequate compaction pressure on $NbSe_3$ electrodes was applied by the Teflon shims between the cell walls and outermost (counter) electrodes, was employed for these studies. The cell was sealed with a Teflon O-ring and a pinch seal. All the cells were cathode limited and contained excess of lithium. Porous polypropylene film, Celgard 3501, was used as the separator and 1.5 M $LiAsF_6$ solution in 2 M MeTHF, which was purified as described in [11], was used as electrolyte.

A.c. and d.c. electrochemical experiments were carried out using a PAR 273 potentiostat and 5301

0021-891X/89 $03.00 + .12

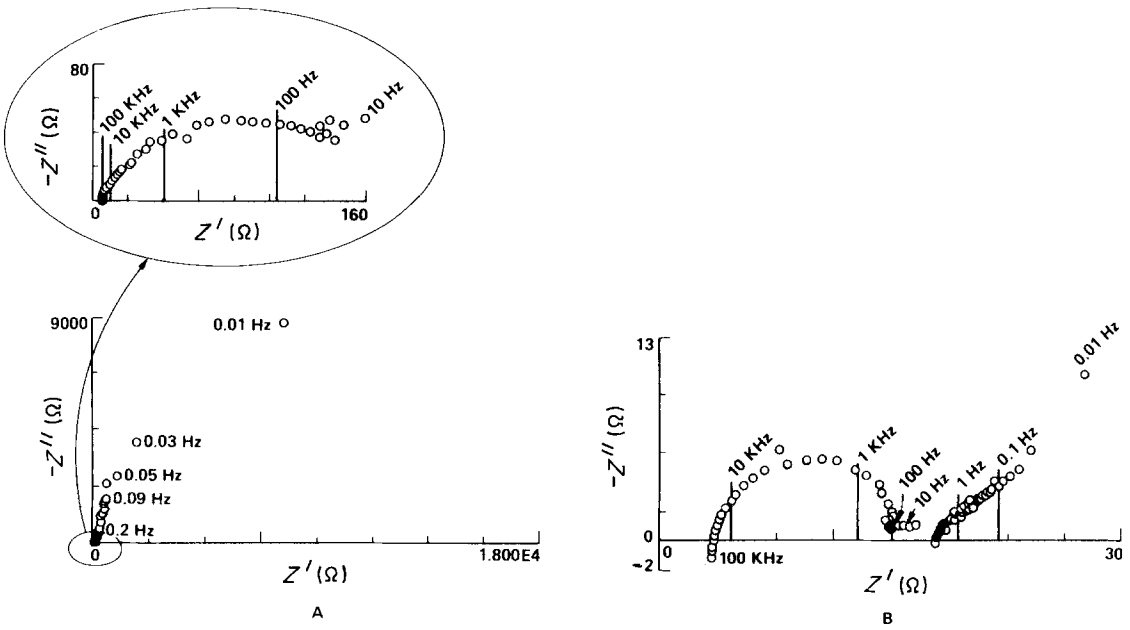

Fig. 1. Typical Nyquist plots of (A) virgin, and (B) partially discharged $NbSe_3$ electrode in 1.5 M $LiAsF_6$/2 M MeTHF solution.

lock-in amplifier interfaced with an Apple IIe computer and with a.c. impedance/SoftCorr software. Charge–discharge cycling of Li–$NbSe_3$ cells was performed with an in-house cycling system interfaced with an IBM-PC.

3. Results and discussion

3.1. *A.c. impedance of virgin $NbSe_3$*

The Nyquist plot of a virgin $NbSe_3$ electrode (Fig. 1) consists of two relaxation loops, the first being much smaller than the other. In the course of discharge of the $NbSe_3$ electrode, the second relaxation loop becomes smaller suggesting that the charge transfer kinetics for the corresponding process becomes faster. These two relaxation loops were attributed to the two charge transfer steps, i.e. intercalation at two different sites involved in the reduction of $NbSe_3$ evidenced from various d.c. and a.c. electrochemical techniques [8]. Assuming a classical Randles equivalent circuit comprising charge transfer resistance and Warburg (diffusion) impedance for each of the intercalation steps, the corresponding kinetic parameters, e.g. exchange current density and Warburg coefficient, were calculated using various graphical methods such as Bode and Randles' plots [12]. The exchange current densities thus obtained for the first and second steps are 97 $\mu A\,cm^{-2}$ and 0.35 $\mu A\,cm^{-2}$, respectively. The exchange current density for the second step is expectedly low at potentials positive to its intercalation potential of ~ 1.7 V. These exchange current densities are strongly dependent on state of charge or the potential of the electrode increasing with a decrease in the latter until the availability of the intercalation sites is maintained.

3.2. *A.c. impedance at different reduction potentials*

A.c. impedance measurements were carried out at various reduction potentials in order to correctly identify the potentials at which the two intercalation steps occur in the potential domain and also to estimate the relative kinetics of these steps at various potentials. The impedance measurements were limited only to the high frequency range (100 kHz–4 Hz) since at lower frequencies, the time of measurements would be longer, during which the electrode might be discharged significantly at these negative potentials and change the nature of the electrode. It is, therefore, possible to obtain only the first relaxation loop in the Nyquist plot which corresponds to the first intercalation step in the reduction of $NbSe_3$.

Figure 2 gives the variation of a.c. impedance of $NbSe_3$ electrode with applied potential at different a.c.

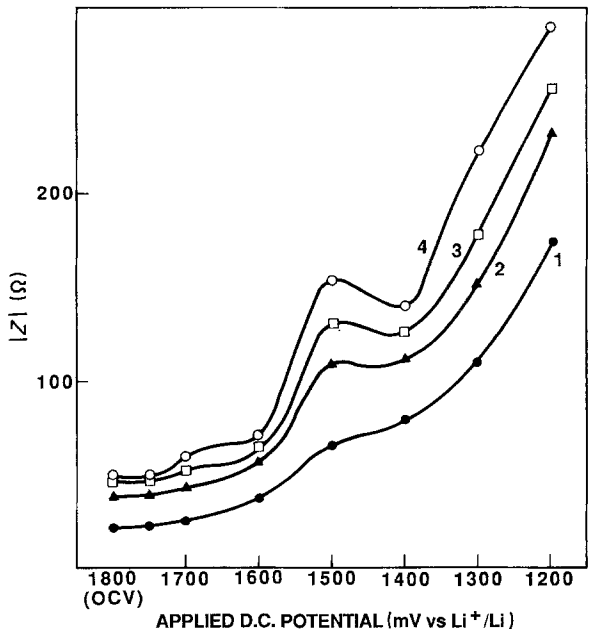

Fig. 2. Variation of impedance of prismatic $NbSe_3$ electrode (area: 2 cm^2) in 1.5 M $LiAsF_6$/2 M MeTHF with applied d.c. potential at an a.c. frequency of (1) 1000 Hz, (2) 316 Hz, (3) 100 Hz, and (4) 10 Hz.

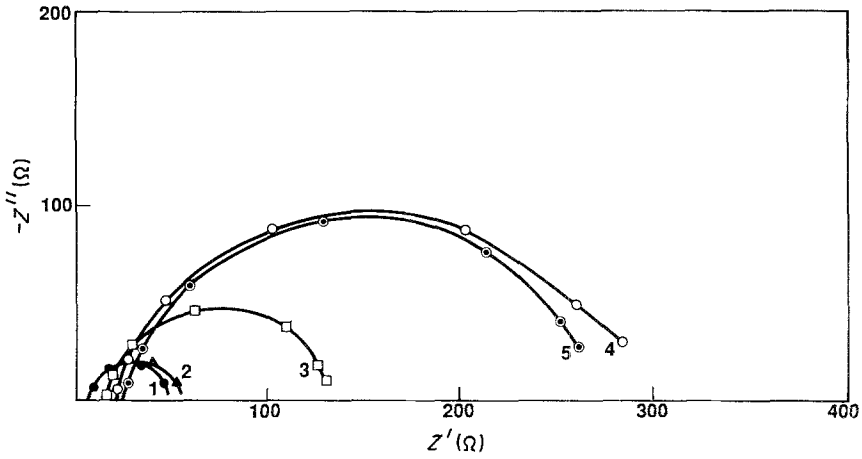

Fig. 3. Nyquist plots of prismatic $NbSe_3$ electrode (area: 2 cm^2) at a d.c. potential of (1) 1.801 V (OCV), (2) 1.70 V, (3) 1.60 V, (4) 1.50 V, and (5) 1.40 V vs Li^+/Li.

frequencies. It may be seen that the impedance of $NbSe_3$ remains constant from OCV ($\sim$ 1.8 V) to 1.75 V and tends to increase therefrom. At a potential $\sim$ 1.70 V, the impedance tends to level off especially at low frequencies and remains the same up to $\sim$ 1.60 V. From our earlier deduction on the mechanism of intercalation of lithium in $NbSe_3$ [8, 10], these variations may be ascribed to the two intercalation steps involved in the reduction of $NbSe_3$. It thus appears from the impedance variations that the first intercalation step ranges from OCV to 1.75 V beyond which its kinetics may be governed by the mass transfer of Li at the corresponding sites. The levelling of impedance between 1.7 and 1.6 V may be due to the second intercalation step being electrochemically (potentially) favored. Beyond 1.60 V, the second step also becomes diffusion limited and hence the increase in the impedance. There is also another sharp hump in the impedance at 1.4 V. However, in view of the large magnitude of the impedance at this potential and also of our earlier observation from coulometric (potentiostatic) titrations that about 2.4 moles of Li is already intercalated to a cut-off potential of 1.55 V, it may be concluded that the hump at 1.4 V is not related to any charge transfer process involving the reduction of $NbSe_3$. Instead, the steady increase in the impedance with a decrease in potential below 1.6 V could be due to an increasing diffusion polarization as a result of high d.c. currents flowing at these potentials and the hump at 1.4 V may be a diffusion-related artifact.

The above a.c. impedance data at different d.c. potentials may be recast into more convenient forms such as Nyquist (Fig.3) and Bode plots to obtain the kinetic parameters. The relaxation loop in the Nyquist plot (Fig. 3), corresponding to the first intercalation step, increases with a decrease in electrode potential. In other words, the charge transfer resistance increases or the apparent exchange current density (Fig. 4) decreases with decreasing d.c. potential. This is contrary to the expectation that the charge transfer (reduction in this case) kinetics becomes faster at lower potentials. However, the kinetics of $NbSe_3$ reduction is essentially governed by the rate of dif-

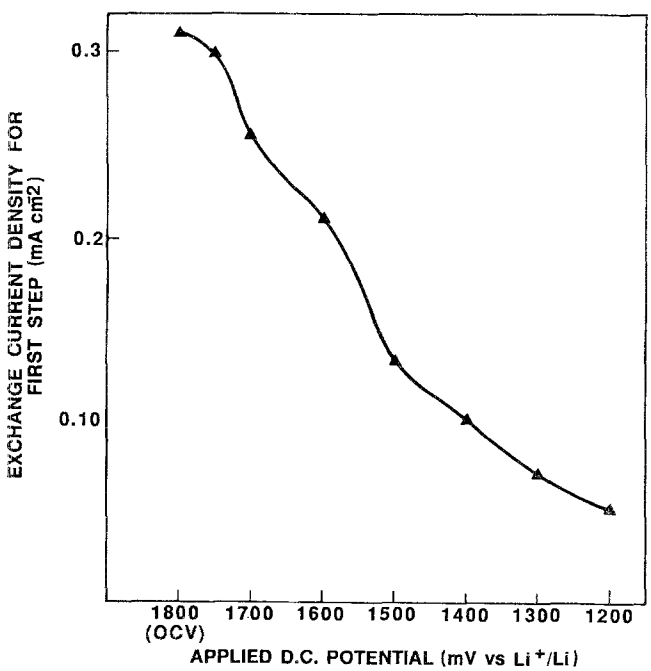

Fig. 4. Variation of exchange current density for the first step in the reduction of $NbSe_3$ electrode with applied d.c. potential.

fusion of Li^+ inside the lattice of $NbSe_3$ as mentioned earlier [8, 10]. Owing to the diffusion-limited kinetics, the interfacial concentration of the reactant species (intercalation sites in this case) decreases at decreasing potentials due to higher d.c. currents (and concentration gradients). The diffusional impedance then becomes a major factor in the electrode impedance. It is thus possible to observe higher values of impedances at increasing overpotentials due to the dominance of mass transfer effects [13]. Under these non-equilibrium conditions, it is difficult to estimate the charge transfer impedance from the total impedance of the electrode to obtain meaningful information on the charge transfer kinetics. Nevertheless, these studies lend further support to the two-step intercalation mechanism in the reduction of $NbSe_3$ and help us locate the potentials for the corresponding steps.

3.3. *A.c. impedance after coulometric discharge at various potentials*

In order to avoid the complications arising out of high d.c. currents flowing across the electrode during a.c. impedance measurements in the above experiment, a different approach was adopted here. The electrode was discharged coulometrically at various potentials, i.e. potentiostatically for long durations until the current reaches a low value. A.c. impedance measurements were then carried out after allowing for equilibrium to set in.

Figure 5 shows the a.c. impedance of the $NbSe_3$ electrode at various a.c. frequencies as a function of potential at which the electrode was discharged

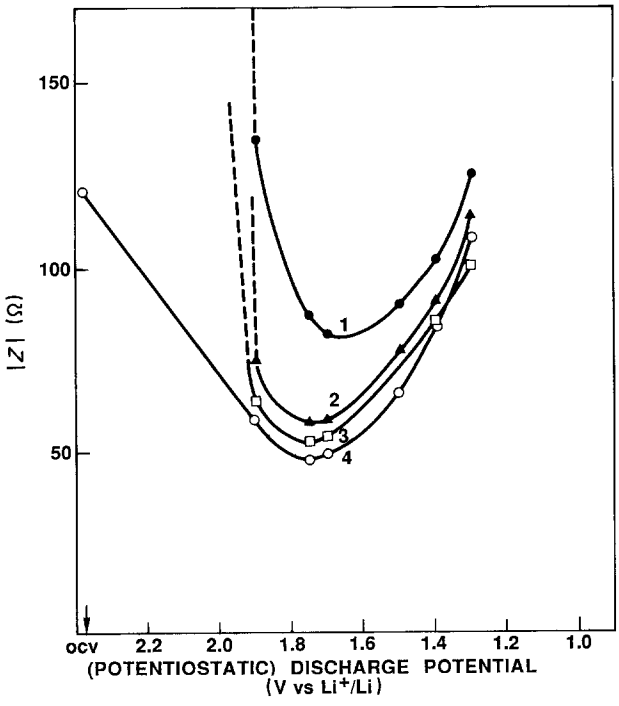

Fig. 5. Variation of impedance of $NbSe_3$ electrode (area: 1 cm^2) at a frequency of (1) 0.01 Hz, (2) 0.1 Hz, (3) 1 Hz, and (4) 10 Hz with d.c. potential at which the electrode was coulometrically discharged prior to a.c. measurements.

coulometrically prior to a.c. measurements. The impedance decreased sharply with a decrease in potential from OCV (~ 2.3) to 1.9 V which may be attributed to the occurrence of the first intercalation step. The impedance continues to decrease and attains a minimum value at 1.7–1.75 V which is a result of the onset of the second intercalation step, as also discussed in Section 3.1. The increase in a.c. impedance therefrom could be attributed to a substantial decrease in the concentration of active species (intercalation sites in this case) due to coulometric discharge. It is interesting to note that the hump in impedance around 1.4 V observed in the above experiment (Section 3.1) is absent in this case thus suggesting that it could only be due to a high d.c. current (diffusion) related artifact.

In the Nyquist form (Fig. 6), the relaxation loop at higher frequencies corresponding to the first intercalation step decreases gradually to 1.75 V, remains the same up to 1.70 V and then increases subsequently. This initial decrease in charge transfer resistance is expected at lower potentials favoring reduction. The increase in the charge transfer resistance below 1.70 V may be due to a significant decrease in the concentration of corresponding intercalation sites during coulometric discharge at $\geqslant 1.7$ V. The second relaxation loop at low frequencies, which is overlapped by diffusion polarization, also decreases with decreasing potential especially at potentials lower than 1.7 V. At potentials $\geqslant 1.7$ V, the charge transfer resistance is orders of magnitude higher than at potentials lower than 1.7 V, which is consistent with our observation that intercalation at sites corresponding to the second step is favored only at potentials $\leqslant 1.7$ V. The charge transfer resistance for the second intercalation step shows a minimum at 1.55 V. The increase in the charge transfer resistance below 1.55 V is once again due to the depletion of the corresponding intercalation sites.

Accordingly, the exchange current densities for the two intercalation steps calculated from Bode and Nyquist plots show an interesting trend (Fig. 7). The exchange current density for the first intercalation step exhibits a peak at 1.75 V suggesting that this could be the mean intercalation potential for the first step. The exchange current density for the second intercalation step, on the other hand, attains a maximum value between 1.7 and 1.5 V, wherein lies the corresponding intercalation potential.

It is thus clear from the above analysis of a.c. impedance after coulometric discharge at various potentials that the reduction of virgin $NbSe_3$ involves two-step intercalation with the intercalation potentials being ~ 100 mV apart which corroborates our earlier deductions from different electrochemical techniques [8, 10].

3.4. *A.c. impedance after cycling*

Laboratory prismatic glass Li–$NbSe_3$ cells of capacity 40 mAh and 30 mAh were subjected to charge–discharge cycling. The cells exhibited good performance early on with a coulombic efficiency of $\sim 90\%$

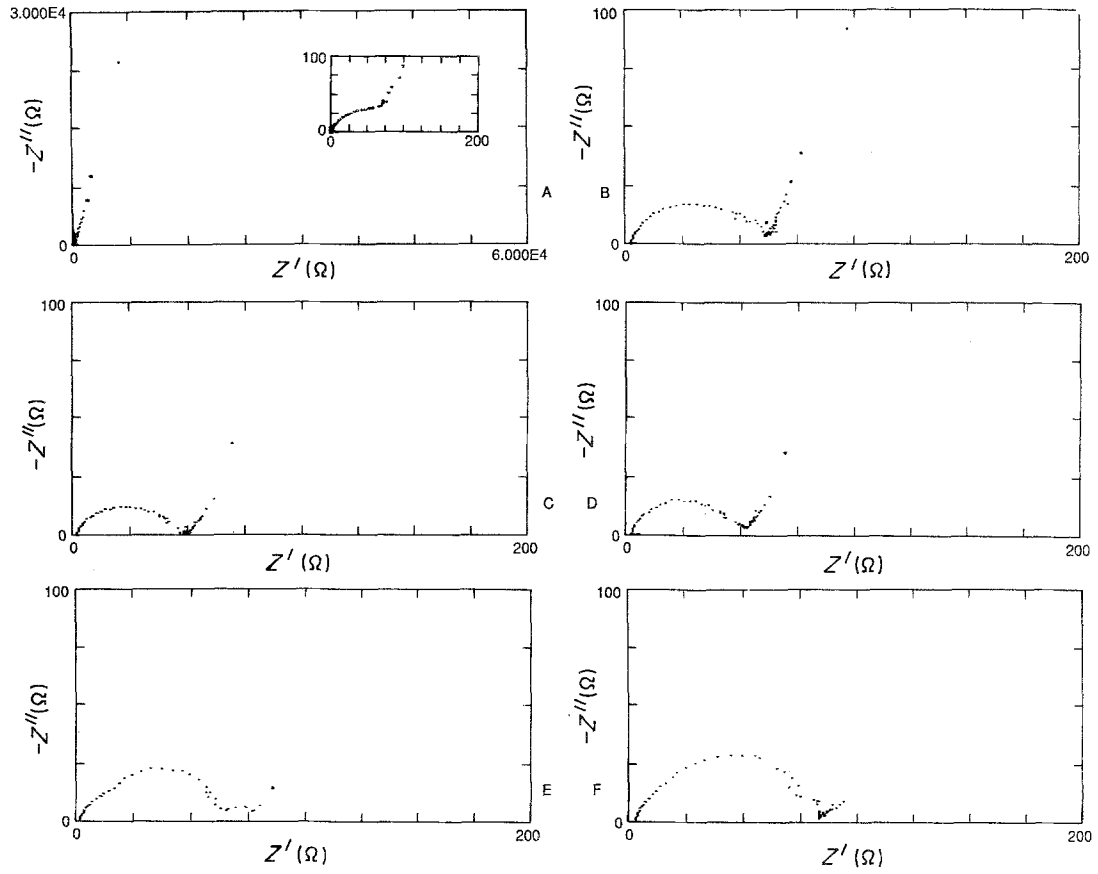

Fig. 6. Nyquist plots of prismatic $NbSe_3$ electrode (area: 1 cm^2) after coulometric discharge at various reduction potentials in 1.5 M $LiAsF_6$/2 M MeTHF solution (a) virgin, (b) 1.9 V, (c) 1.75 V, (d) 1.70 V, (e) 1.55 V, and (f) 1.4 V.

but suffered 'capacity loss' within 10 cycles, the loss being too abrupt to attribute to any component/electrode failure. This was identified to be due to a loss of solvent, 2 M MeTHF, by evaporation through the non-hermetic seal, from the electrolyte thus drying up the cell and increasing its internal resistance. These cells were rejuvenated by adding solvent. After 'reactivation' by solvent addition, the cells regained their original capacities.

Figure 6 gives a comparison of the impedance spectra of a typical dried cell before and after solvent addition. It should be mentioned here that the a.c. impedance spectrum of $NbSe_3$ changes considerably on charge–discharge cycling. The second relaxation loop, observed at low frequencies, gradually vanishes, probably merging with the first arc at high frequencies. In other words, it is not possible to distinguish the two discrete steps, if any, by any of the electrochemical techniques adopted, i.e. a.c. and d.c. cyclic voltammetry, coulometric titrations, a.c. impedance, etc. This is related to the structural change occurring in $NbSe_3$ on lithiation (charge–discharge cycling) making it 'amorphous', which might smooth out the structural dissimilarities between the two types of intercalation sites [8]. The a.c. impedance (Nyquist plot) of cycled $NbSe_3$ thus typically consists of a high frequency relaxation loop corresponding to charge transfer processes and a low frequency linearity corresponding to the slow diffusional processes of Li^+ inside the cathode. The impedance spectrum before solvent addition shows an irregular and ill-defined pattern with considerable scatter, especially at low frequencies. Also, the impedance is, in general, one or more orders of magnitude higher than in reactivated cells. It is thus clear that, with the help of the a.c. impedance technique, it is possible to diagnose the cell

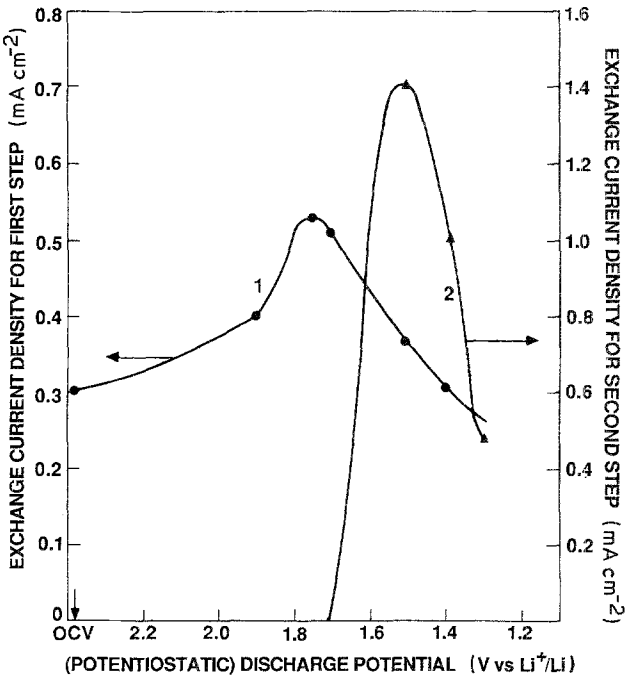

Fig. 7. Variation of exchange current densities for the (1) first step, and (2) second step in the reduction of $NbSe_3$ electrode with the d.c. potential at which the electrode was coulometrically discharged prior to a.c. measurements.

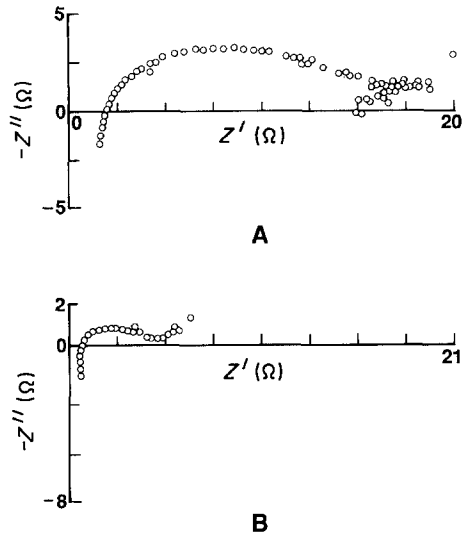

Fig. 8. Impedance spectra of a prismatic 40 mAh Li–$NbSe_3$ glass cell: (A) failed due to evaporation of solvent 2 M MeTHF through non-hermetic seal, and (B) rejuvenated by adding 2 M MeTHF.

failure due to loss of electrolyte. Such a situation is likely to be encountered in any lithium rechargeable battery due to the unavoidable reaction between the electrolyte and lithium anode especially in starved-electrolyte or electrolyte-limited designs. Consumption of lithium by this side reaction is not a serious concern since it is usually in excess over the cathode but the loss of electrolyte which may be identified by a.c. impedance technique is certainly a deterrent factor in the performance of the cell.

4. Conclusions

A.c. impedance measurements at different d.c. potentials, as well as after coulometric discharge at various potentials, thus support our earlier findings that the intercalation of 3 moles of Li with $NbSe_3$ occurs in two steps, the potentials of which are closely spaced yet noticeably apart. Finally, a.c. impedance techniques may be adapted to diagnose failure modes of Li–$NbSe_3$ cells on cycling/storage.

Acknowledgement

The work described here was carried out at the Jet Propulsion Laboratory, California Institute of Technology, under contact with the National Aeronautics and Space Administration. One of the authors (B. V. Ratnakumar) acknowledges the National Research Council for providing his Research Associateship during this work. We would also like to thank Dr G. Nagasubramanian for very helpful discussions.

References

[1] J. Broadhead, F. J. Di Salvo and F. A. Trumbore, U. S. Patent 3, 864, 167 (1975).
[2] D. W. Murphy and F. A. Trumbore, *J. Electrochem. Soc.* **123** (1976) 960; *J. Crystal Growth* **39** (1977) 185.
[3] J. N. Carides and D. W. Murphy, *J. Electrochem. Soc.* **124** (1977) 1309.
[4] J. Broadhead, F. A. Trumbore and S. Basu, *J. Electroanal. Chem.* **118** (1981) 241.
[5] M. S. Whittingham and G. H. Newman, *J. Electrochem. Soc.* **128** (1981) 706.
[6] N. Kumugai, K. Tanno and N. Kumugai, *Denki Kagaku* **49** (1981) 567.
[7] B. V. Ratnakumar, C. L. Ni, S. Di Stefano, R. B. Somoano and C. P. Bankston, Proc. Symposium on Lithium Batteries, Publication 88-6 The Electrochemical Society, NJ (1988) p. 565.
[8] B. V. Ratnakumar, C. L. Ni, S. Di Stefano, G. Nagasubramanian and C. P. Bankston, *J. Electrochem. Soc.*, in press.
[9] J. L. Hodeau, M. Marezio, C. Roucau, R. Ayroles, A. Meershaut, J. Rouxel and P. Monceau, *J. Phys. C., Solid State Phys.* **11** (1978) 4117.
[10] B. V. Ratnakumar, S. Di Stefano and C. P. Bankston, 33rd International Power Sources Symposium, Cherry Hill, NJ, June 13–16 (1988).
[11] D. H. Shun, S. P. S. Yen, B. J. Carter and R. B. Somoano, Proc. ECS Symposium on Lithium Batteries, Publication 84-1, The Electrochemical Society, NJ (1983).
[12] D. D. MacDonald, 'Transient Techniques in Electrochemistry', Plenum Press, New York (1977).
[13] B. B. Damaskin, 'The Principles of Current Methods for the Study of Electrochemical Reactions', McGraw-Hill, New York (1967).